UNIVERSIDAD REGIONAL AMAZÓNICA IKIAM

FACULTAD DE CIENCIAS DE VIDA

CARRERA DE BIOTECNOLOGÍA

FUNCTIONALIZATION OF HEMP CELLULOSE WITH BIOI MICROSPHERES BY HOT-PRESSING FOR THE PHOTOCATALYTIC DEGRADATION OF METHYLENE BLUE

Proyecto de investigación previo a la obtención del Título de:

INGENIERA EN BIOTECNOLOGÍA

AUTORA

KERLY JAMILETH DÍAZ SOLÓRZANO

Tena – Ecuador

2025

UNIVERSIDAD REGIONAL AMAZÓNICA IKIAM

FACULTAD DE CIENCIAS DE VIDA

CARRERA DE BIOTECNOLOGÍA

FUNCTIONALIZATION OF HEMP CELLULOSE WITH BIOI MICROSPHERES BY HOT-PRESSING FOR THE PHOTOCATALYTIC DEGRADATION OF METHYLENE BLUE

Proyecto de investigación previo a la obtención del Título de:

INGENIERA EN BIOTECNOLOGÍA

AUTOR: KERLY JAMILETH DÍAZ SOLÓRZANO

TUTOR: Mgs. LUIS MIGUEL QUISHPE QUISHPE

CO-TUTOR: Ph.D MIGUEL HERRERA ROBLEDO

Tena – Ecuador

2025

Carrera de Biotecnología

Declaración de derecho de autor, autenticidad y responsabilidad

Tena, 17 de marzo del 2025

Yo, Kerly Jamileth Díaz Solórzano, con documento de identidad 2150219679, declaro que los resultados obtenidos en la investigación que presento en este documento final, previo a la obtención del título de Ingeniería en Biotecnología, son absolutamente inéditos, originales, auténticos y personales.

En virtud de lo cual, el contenido, criterios, opiniones, resultados, análisis, interpretaciones, conclusiones, recomendaciones y todos los demás aspectos vertidos en el presente documento, son de mi autoría y de mi absoluta responsabilidad.

Kerly Jamileth Díaz Solórzano

CI: 2150219679

Carrera de Biotecnología

Autorización de publicación en el repositorio institucional

Tena, 17 de marzo del 2025

Yo, Kerly Jamileth Díaz Solórzano, con documento de identidad 2150219679 en calidad de autor/a y titular de los derechos morales y patrimoniales del trabajo de titulación "Functionalization of hemp cellulose with BiOI microspheres by hot-pressing for the photocatalytic degradation of methylene blue." de conformidad con el Art. 114 del CÓDIGO ORGÁNICO DE LA ECONOMÍA SOCIAL DE LOS CONOCIMIENTOS, CREATIVIDAD E INNOVACIÓN, reconozco a favor de la Universidad Regional Amazónica Ikiam una licencia gratuita, intransferible y no exclusiva para el uso no comercial de la obra, con fines estrictamente académicos.

Así mismo autorizo a la Universidad Regional Amazónica Ikiam para que realice la publicación de este trabajo de titulación en el Repositorio Institucional de conformidad a lo dispuesto en el Art. 144 de la Ley Orgánica de Educación Superior.

Atentamente,

Kerly Jamileth Díaz Solórzano

CI: 2150219679

Carrera de Biotecnología

Certificado de dirección de trabajo titulación

Tena, 17 de marzo del 2025

Certifico que el trabajo de titulación: “Functionalization of hemp cellulose with BiOI microspheres by hot-pressing for the photocatalytic degradation of methylene blue.”, aprobado bajo el mecanismo de titulación de: artículo, fue realizado por Kerly Jamileth Diaz Solorzano, bajo mi dirección.

El mismo ha sido revisado en su totalidad y analizado por la herramienta de verificación de similitud de contenido; por lo tanto, cumple con los requisitos teóricos, científicos, técnicos, metodológicos y legales establecidos por la Universidad Regional Amazónica Ikiam, para su entrega y defensa.

Firmado electrónicamente por:
LUIS MIGUEL QUISHPE QUISHPE

Luis Miguel Quishpe Quishpe

CI: 1500843048

Tutor

Firmado electrónicamente por:
MIGUEL HERRERA ROBLEDO

Miguel Herrera Robledo

CI: 1550516452

Cotutor

AGRADECIMIENTOS

Quiero agradecer a mi familia, por su apoyo incondicional y su constante motivación a lo largo de este proceso. Asimismo, agradezco a mi tutor, el profesor Miguel Quishpe, por su guía y dedicación en la dirección de este proyecto. Finalmente, a mis amigos María José y Leonardo Proaño, quienes han sido un pilar fundamental, brindándome su amistad y su colaboración en momentos clave.

.

DEDICATORIA

Dedico este trabajo a mi familia, de manera especial a mi mamá Maribel, a mi hermana Daniela y a los trillizos. A mis amigos, María José, Leonardo Proaño, Aleydis, Willy y Andrés por todo el apoyo y amistad. A mis gatitos, Dorito y Blanca. Finalmente, a mi papá, Patricio y a mi querido amigo Alejandro. Siendo sincera, en el proceso de este trabajo hubo momentos de dudas sobre mi capacidad. Sin embargo, recordarlos me dio la fuerza para continuar. Gracias por los regaños y las palabras de apoyo que alguna vez tuve la fortuna de recibir. Aunque ya no puedo verlos, realmente aún siento su cariño inmenso.

TABLA DE CONTENIDO

ÍNDICE DE FIGURAS

RESUMEN

Esta investigación se centra en la problemática de la contaminación acuática por colorantes industriales, con especial énfasis en el azul de metileno (AM), un contaminante persistente y tóxico. Se planteó la funcionalización de las membranas de celulosa de cáñamo con microesferas de oxiyoduro de bismuto (BiOI) a través de prensado en caliente, con el objetivo de optimizar la eficiencia en la degradación fotocatalítica de la celulosa de cáñamo. Las microesferas de BiOI fueron sintetizadas mediante un procedimiento solvotermal y se caracterizaron a través de la difracción de rayos X (XRD), la espectroscopía de energía dispersiva de rayos X (EDS) y la microscopía electrónica de barrido (SEM). Los hallazgos señalan que las membranas funcionalizadas con BiOI exhibieron una eficiencia superior en la degradación de AM bajo luz visible, logrando hasta un 93.67% de eliminación con la concentración óptima de BiOI. Sin embargo, el aumento de la dosis de BiOI provocó un efecto de saturación, reduciendo la eficiencia. Estos resultados ponen de relieve el potencial de las membranas de celulosa de cáñamo funcionalizadas con BiOI como solución sostenible y eficaz para el tratamiento de aguas residuales en aplicaciones industriales.

Palabras Clave: Celulosa, Cáñamo, Fotocatálisis, Funcionalización, BiOI, Azul de metileno

ABSTRACT

This investigation focuses on the problem of aquatic pollution by industrial dyes, with special emphasis on methylene blue (MB), a persistent and toxic pollutant. The functionalization of hemp cellulose membranes with bismuth oxyiodide (BiOI) microspheres through hot pressing was proposed, with the aim of optimizing the efficiency in the photocatalytic degradation of hemp cellulose. The BiOI microspheres were synthesized through a solvothermal procedure and characterized through X-ray diffraction (XRD), energy dispersive X-ray spectroscopy (EDS) and scanning electron microscopy (SEM). The findings indicate that the BiOI-functionalized membranes exhibited superior AM degradation efficiency under visible light, achieving up to 93.67% removal at the optimal BiOI concentration. However, increasing BiOI dosage led to a saturation effect, reducing efficiency. These findings highlight the potential of BiOI-functionalized hemp cellulose membranes as a sustainable and effective solution for wastewater treatment in industrial applications.

Keywords: Cellulose, Hemp, Photocatalysis, Functionalization, BiOI, Methylene Blue-

Journal of Environmental Chemical Engineering

Link: https://www.sciencedirect.com/journal/journal-of-environmental-chemical-engineering/publish/guide-for-authors

Functionalization of hemp cellulose with BiOI microspheres by hot-pressing for the photocatalytic degradation of methylene blue

Kerly Díaz[a]

[a]Universidad Regional Amazónica Ikiam, Muyuna Road km 7, San Juan de Tena, Napo, Ecuador.

1. INTRODUCTION

Water is an essential resource for all living organisms. However, the presence of cationic organic dyes, such as methylene blue (MB), in water effluents has raised significant concerns due to their harmful effects on human health and the environment (Ekeoma et al., 2023; Patel et al., 2020). This compound is widely used in various textile and plastic industries, which produce between 10% and 15% of wastewater; MB is the main pollutant and is highly visible even in small amounts (< 1 ppm). In this sense, its uncontrolled release can compromise water quality due to its toxicity and persistence in the environment (Ara & Ghafuri, 2024; Ekeoma et al., 2023; Fito et al., 2020, 2023; Hashem et al., 2020; Patel et al., 2020; Santoso et al., 2020; Sivakumar & Lee, 2022). Previous studies have evidenced that MB can induce detrimental health effects in humans, including nausea, vomiting, and cardiac arrhythmias. Furthermore, MB has been shown to negatively impact aquatic ecosystems by disrupting biodiversity and ecological balance (Ara & Ghafuri, 2024; Oladoye et al., 2022; Sivakumar & Lee, 2022). For this reason, it is necessary to develop efficient water treatment methods to eliminate MB.

The effective removal of organic dyes from wastewater has been carried out with technologies such as adsorption, ultrafiltration, advanced oxidation, and co-precipitation (S. Khan et al., 2022; Negrete-Bolagay et al., 2021; Oladoye et al., 2022; Santoso et al., 2020; Sivakumar & Lee, 2022). Among them, adsorption technologies stands out for their high efficiency and low cost (Candamano et al., 2023; Kausar et al., 2023). In particular, cellulose-based technologies have emerged as a potential alternative due to its great abundance in the nature, biodegradability, and the presence of hydroxyl groups (-OH), which facilitate the adsorption of contaminant dyes (Akköz & Coşkun, 2023). Owing to these facts, the production of various cellulose forms from hemp has been explored because their fibers exhibit attractive properties for water treatment, including high mechanical strength, stiffness, and roughness (Tofan et al., 2020). Among the structural forms of cellulose, nanofibrillated cellulose (NFC) and nanocrystalline cellulose (NCC) have proven to be particularly effective in the removal of

contaminants (Mahfoudhi & Boufi, 2017). NFC has been successfully used in the elimination of MB and toluidine blue, while NCC has shown efficacy in the adsorption of dyes such as acid red, K-4G yellow, and Congo red (Basak et al., 2015; Mahfoudhi & Boufi, 2017). However, their practical application is still limited due to the saturation of their active sites after several cycles of use, which demands post-treatments with high energy consumption for the release of the contaminant and their regeneration. Therefore, enhancing cellulose properties is essential to lowering water treatment costs and increasing the remotion efficiency of the target contaminants (Hokkanen et al., 2016).

The incorporation of photocatalytic semiconductor materials into cellulose has emerged as a promising alternative to enhance its functionality and go beyond an adsorption material (S. Khan et al., 2022). These materials possess the capacity to degrade organic compounds by generating reactive oxygen species (ROS) under light irradiation (Houas et al., 2001). In recent years, bismuth oxyhalides (BiOX, where X = Br, Cl, I) have intensively studied as a novel class of promising materials for photocatalytic energy conversion and environmental remediation (Di et al., 2017). Based on the aforementioned, different composited based on cellulose and bismuth oxyhalide-based photocatalysts have been developed. For example, BiOBr/RC (M. Du et al., 2018) and BiOCl/NCC (Wang et al., 2022) composited have shown a high capacity to remove and degrade Rhodamine B (RhB). Likewise, the preparation of BiOBr/BiOI/Cellulose composites capable of removing and degrading dyes (e.g., Rhodamine B and fluorescent dye has been reported (M. Du et al., 2019; Xu et al., 2023).

However, their application has been restricted because both BiOCl and BiOBr have a wide band gap of approximately 3.3 and 2.64 eV, respectively (Li et al., 2021). This band gap prevents them from fully utilizing visible light. BiOCl exhibits a high absorption capacity only with UV light, which corresponds to 5% of the solar spectrum. In real applications it is important that semiconductor materials can absorb photons of visible light (45% of the solar spectrum) to have higher efficiency (Oladoye et al., 2022). BiOBr, although it has a narrower bandgap allowing it to work with visible light, faces a limitation as a semiconductor due to the high recombination rate of photogenerated

electron-hole pairs and the low efficiency of light absorption (Onwumere et al., 2020). In this sense, bismuth oxyiodide (BiOI) semiconductor-based materials have been studied as potential candidates to improve cellulose properties. This is because BiOI exhibits a narrow band gap (1.73-1.92 eV), which allows it efficiently absorbing photons in the visible light range. Moreover, due to its crystalline structure which is composed of alternating layers of $[Bi_2O_2]^{2+}$ ions and halogens $[I^-]$ atoms, it can promote efficiently the separation of charge carriers, increasing the production of ROS (reactive oxygen species) and its capacity to degrade contaminants (Zuarez-Chamba et al., 2022). Nevertheless, to date, the development of hemp cellulose membranes functionalized with BiOI microspheres for the removal of methylene blue (MB) has not been reported.

Therefore, the general aim of the present work is to evaluate the efficiency of hemp cellulose membranes functionalized with BiOI microspheres in the removal and degradation of methylene blue. To achieve this, the specific objectives are (1) to synthesize BiOI microspheres via a solvothermal method, (2) to functionalize hemp cellulose membranes with BiOI microspheres, and (3) to evaluate the efficiency of functionalized hemp cellulose membranes in the removal and degradation of methylene blue under white LED light irradiation.

2. MATERIALS AND METHODS

2.1. Materials and reagents

All reagents were analytical grade and used as received without further treatment. Bismuth (III) nitrate pentahydrate ($Bi(NO_3)_3 \cdot 5H_2O$, Sigma-Aldrich, ≥98%), potassium iodide (KI, ExiPlus, Multi-Compendial, 99.8%) and ethylene glycol ($C_2H_4(OH)_2$, Sigma-Aldrich, ≥99%) were used for the synthesis of BiOI microspheres. Functionalized hemp cellulose samples were supplied by the research group of Frank Alexis at Universidad San Francisco de Quito. Methylene Blue (MB) was used as a model pollutant and ultrapure water was used in batch experiments.

2.2. Synthesis of BiOI flower-like microspheres

The synthesis of BiOI microspheres was performed by a solvothermal method described by Zuarez-Chamba et al. (2022) with some modifications to the temperature and reaction time. For this, a solution A was prepared by dissolving 3 mmol of ($Bi(NO_3)_3 \cdot 5H_2O$) in 30 mL of ethylene glycol with sonication for 30 min, followed by constant stirring (500 rpm) for 30 min. At the same time, a solution B was prepared by dissolving 3 mmol of KI in 30 mL of ethylene glycol under continuous stirring (500 rpm) for 30 min. Then, solution B was added dropwise (1 mL/min) to solution A under constant stirring (500 rpm). The solution was left under constant stirring (500 rpm) for 30 min and transferred to a 100 mL Teflon-lined autoclave. The autoclave was placed in a stainless-steel reactor and heated in an oven at 160 °C for 3 h. The reactor was then allowed to cool at room temperature. Subsequently, the precipitate was collected by vacuum filtration with a nylon membrane with a pore size of 0.22 µm and washed with deionized water, followed by ethanol (96%) and finally with deionized water. The precipitate obtained was dried at 60 °C for 4 h.

2.3. Functionalization of hemp-based cellulose membranes with BiOI microspheres

Functionalization of the hemp-based cellulose membranes was performed with different dosages of BiOI microspheres (0.1, 0.2 y 0.4 mg BiOI/mg cellulose) using the following procedure: first, 0.02 mL of distilled water was added for each mg of cellulose. Then, the samples were taken to a heating plate at 100 °C for 30 min. Finally, the membranes were prepared by distributing 250 mg of the mixture on a thermo-resistant paper, which were subsequently subjected to a thermo-pressing method (hot-pressing) at 115.55 °C and a pressure of 40 MPa for 4 min using the 20-ton Rosin Press Dabpress equipment (Chen et al., 2020). The resulting samples were labeled HC/BiOI-0, HC/BiOI-50, HC/BiOI-100 and HC/BiOI-200, corresponding to the different doses of BiOI microspheres used in the functionalization process, where HC/BiOI-0 indicates no BiOI added, HC/BiOI-50 represents the addition of 50 mg BiOI, HC/BiOI-100 corresponds to 100 mg BiOI and HC/BiOI-200 reflects the highest dose of 200 mg BiOI.

2.4. Structural, chemical and morphological characterization

The crystallinity of the samples was performed by X-ray Diffraction (XRD) on a Malvern Panalytical Empyrean X-ray diffractometer equipped with a copper X-ray tube (Kα radiation, λ = 1.54056 A°). The morphology of the materials was observed by Scanning Electron Microscopy (SEM) on a Tescan Mira 3 scanning electron microscope. For SEM observation, the cellulose membranes and functionalized membranes were first dried by lyophilization and sputter coated with Pt. Analysis of SEM images were performed with the ImageJ software. Finally, the chemical composition was determined by Energy Dispersive X-ray Spectroscopy (EDS) using a Bruker X-Flash 6-30 detector coupled to SEM equipment, with a resolution of 123 eV at Mn Kα. Additionally, to study more about BiOI and hemp cellulose crystal properties, the average crystal size value was calculated using the Debye–Scherrer equation (Bokuniaeva & Vorokh, 2019) and the crystallinity index (CrI) was calculated according to Hermans (Hermans & Weidinger, 1948):

$$L = \frac{K\lambda}{\beta cos\theta}$$

$$CrI = \frac{A_{cryst}}{A_{total}} \times 100$$

Where L represents the crystallite size, K (0.9) is a constant, λ (0.15418 nm) is the wavelength of X-rays, β is the FWHM (full width at half maximum; in radian), and θ is the Bragg angle. In the case of crystallinity index (CrI), A_{cryst} is the sum of crystalline band areas and A_{total} is the total area under the diffractograms.

2.5. Photocatalytic evaluation

The evaluation of the photocatalytic activity and removal efficiency of functionalized cellulose membranes was performed by degrading 3 mg/L MB in solution under visible light. For this, a photoreactor equipped with two fans, a 250 mL beaker, a stirring plate and a white light LED lamp (150 W, 15000 Lm, 6200 K, 90-265 V) placed at 33 cm from the beaker were used. Batch experiments were conducted under visible light and darkness. Then, 100 mg of each functionalized hemp cellulose membrane HC/BiOI-0, HC/BiOI-50, HC/BiOI-100 and HC/BiOI-200 was immersed in 100 mL of MB solution and stirred at 400 rpm for 1 h both under dark conditions and visible light. An initial aliquot was taken from the stock solution before starting the experiment to determine the initial concentration at 0 min, and a second aliquot of 10 mL was taken at the end of the exposure period (Figueroa, 2020). In addition, tests with unfunctionalized hemp cellulose, different amounts of BiOI (50, 100 and 200 mg), and a photolysis assay were carried out for comparative purposes. Finally, the concentration of MB was measured using a UV-Vis-NIR spectrophotometer (Shimadzu) at 664 nm. Treatments were performed in triplicate (x3) to ensure statistical reliability. Therefore, a one-way Analysis of Variance (ANOVA) was used for statistical analyses, with a significance level set at $p < 0.05$. The software RStudio was used to perform statistical analyses and graphical representations.

3. RESULTS AND DISCUSSION

3.1. Instrumental Characterization

3.1.1. XRD

The X-ray diffraction patterns of HC/BiOI-0, HC/BiOI-50, HC/BiOI-100, and HC/BiOI-200 are presented in Fig. 1. Three characteristic peaks are identified in the XRD pattern of HC/BiOI-0 placed at 2θ: 14.902°, 16.494° and 22.842°, which correspond to the crystal planes (1 1 0), (1 -1 0) and (2 0 0), respectively, of cellulose type I (ICDD # 00-003-0289). These results correlate with those reported by Gordon-Falconí et al. (2024) and Du et al. (2024). Moreover, the average crystallite size of HC/BiOI-0 was 4.55 nm (45.5 Å), consistent with the findings of Bolio et al. (2011), who reported an average crystallite size of 4.46 nm. Furthermore, the crystallinity index of HC/BiOI-0 was determined to be 75.08%, similar to the reported in other works (Du et al., 2024). Moreover, the low crystallinity has been attributed to the presence of residual hemicellulose (Du et al., 2024).

On the other hand, when the sample was functionalized with BiOI microspheres new peaks appear in the range of 10° to 80°. As is shown Fig. 1, the diffraction peaks of HC/BiOI-50, HC/BiOI-100 and HC/BiOI-200 located at 2θ: 9.657°, 24.29°, 29.254°, 31.648°, 33.163°, 37.051°, 45.366°, 49.767°, 54.898° and 66.099° are well indexed to the crystallographic planes (0 0 1), (0 1 1), (0 1 2), (1 1 0), (1 1 1), (1 1 2), (0 2 0), (0 2 2), (1 2 2) and (0 2 0) of the tetragonal phase of BiOI (ICDD # 98-039-1354), with a *P4/nmm* space group, and lattice constants of a = b = 3.985 Å and c = 9.129 Å. These findings are consistent with the reported by Zuarez-Chamba et al. (2022).

The crystallite sizes of the microspheres in HC/BiOI-50, HC/BiOI-100, and HC/BiOI-200 samples were determined to be 7.71, 6.88, and 7.69 nm, respectively. Moreover, XRD analysis reveals that as the dosage of BiOI increases from 0 to 200 mg, the intensity of (012), (110), (020), (122) crystallographic planes of BiOI also increases, suggesting a

successful impregnation of microspheres inside the matrix of hemp cellulose membranes. On the other hand, the hemp cellulose peaks corresponding to the crystallographic planes (110) and (200) appear to attenuate as the dosage of BiOI increases, indicating a possible decrease in cellulose crystallinity. This is further supported by the CI values obtained from the cellulose peaks, in which the CI dropped from 75.08% for HC/BiOI-0 to 36.25%, 35.57% and 32.72% for HC/BiOI-50, HC/BiOI-100, and HC/BiOI-200, respectively. This reduction in crystallinity indices is associated with decreasing cellulose crystallite sizes (Poletto et al., 2014).

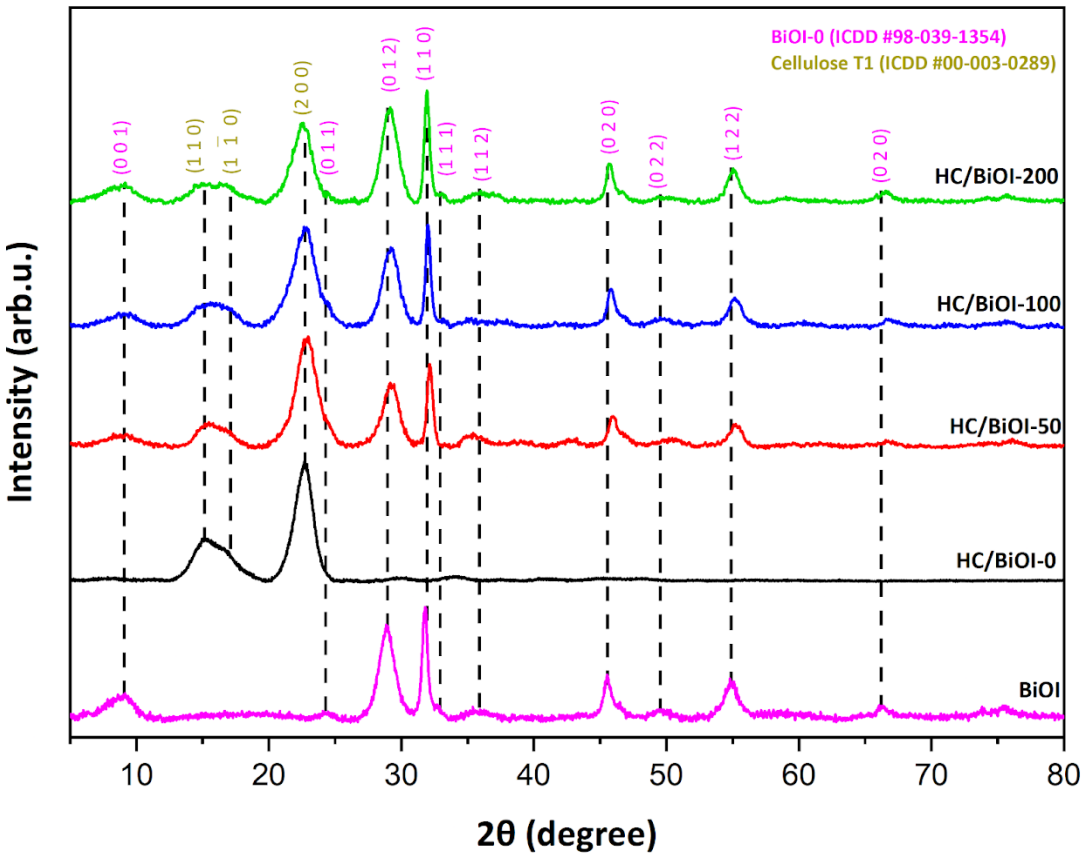

Fig. 1. XRD patterns of BiOI, HC/BiOI-0, HC/BiOI-50, HC/BiOI-100 and HC/BiOI-200 samples.

3.1.2 Morphology and chemical characterization

The morphological characteristics of the prepared samples were analyzed using scanning electron microscopy. As is displayed in Fig. 2a, the HC/BiOI-0 sample exhibits an irregular and fibrous surface composed of pores with an average diameter of approximately 2.840 ± 0.122 µm. On the other hand, the cellulose fibers have an average diameter of approximately 13.270 ± 0.261 µm and a length of 358.815 ± 10.717 µm. Fig. 2b-d presents the SEM images of HC/BiOI-50, HC/BiOI-100, and HC/BiOI-200 samples, respectively. In all the samples, the irregular and fibrous texture of the cellulose membrane is maintained after the functionalization with BiOI microspheres, which have an average diameter approximately of 1.476 ± 0.008 µm. In the case of HC/BiOI-50 and HC/BiOI-100 samples, the distribution of BiOI microspheres is relatively uniform across the sample surface, and some cellulose fibers partially enwrap the microspheres. This is consistent with the observations of Nor et al. (2016), who also reported the partial coverage of TiO_2 particles by membranes nanofibers due to the hot-pressing process.

In contrast, the HC/BiOI-200 sample exhibits a heterogeneous distribution of microspheres on the cellulose matrix and greater agglomeration in different regions of the material. Furthermore, partial coverage of the photocatalytic material by the cellulose fibers is evident. However, some morphological changes of the microspheres are observed, including irregular structures and dispersed fragments across the cellulose surface. Although the hot-pressing technique is characterized by maintaining the morphological integrity of the photocatalysts (Mohamed et al., 2017). These findings suggest that the applied temperature or pressure conditions could have influenced the morphological alterations observed in the BiOI microspheres.

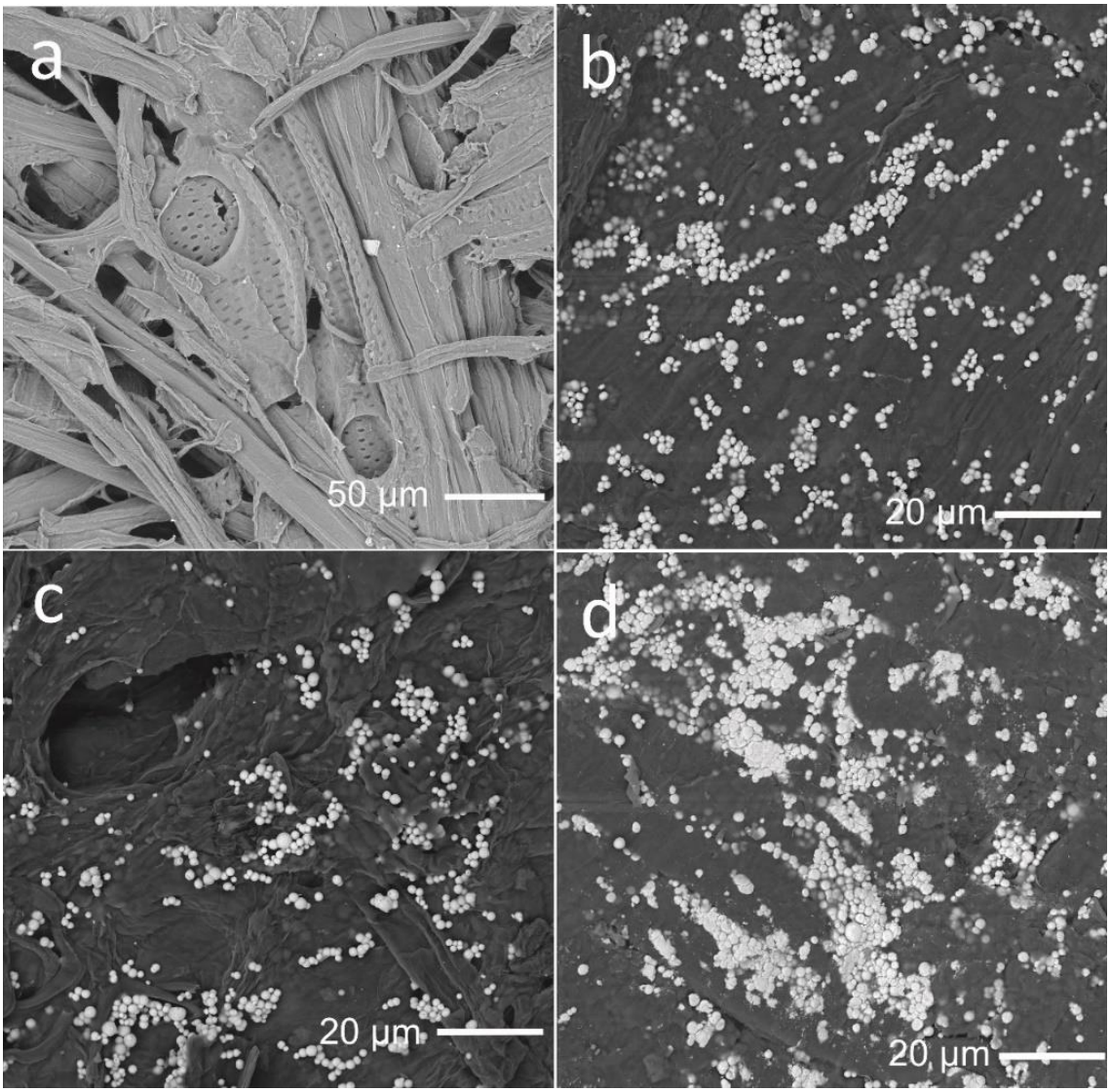

Fig. 2. SEM images of (a) HC/BiOI-0, (b) HC/BiOI-50, (c) HC/BiOI-100 and (d) HC/BiOI-200 samples.

On the other hand, EDS analysis was performed to examine the chemical composition. As shown in Fig. 3a, the hemp cellulose primarily contains carbon (C), oxygen (O), and trace amounts of sodium, chlorine, and calcium. The presence of Na and Cl in the elemental composition of HC/BiOI-0 may originate from the alkaline treatment and bleaching process. For the functionalized samples, as depicted in Fig. 3b-d, peaks attributed to bismuth (Bi), oxygen (O), and iodine (I) are detectable, indicating the presence of synthesized BiOI microspheres. Furthermore, this was confirmed by elemental distribution maps presented in Fig. S2-4, which shows the distribution of Bi, O, and I in all the functionalized samples.

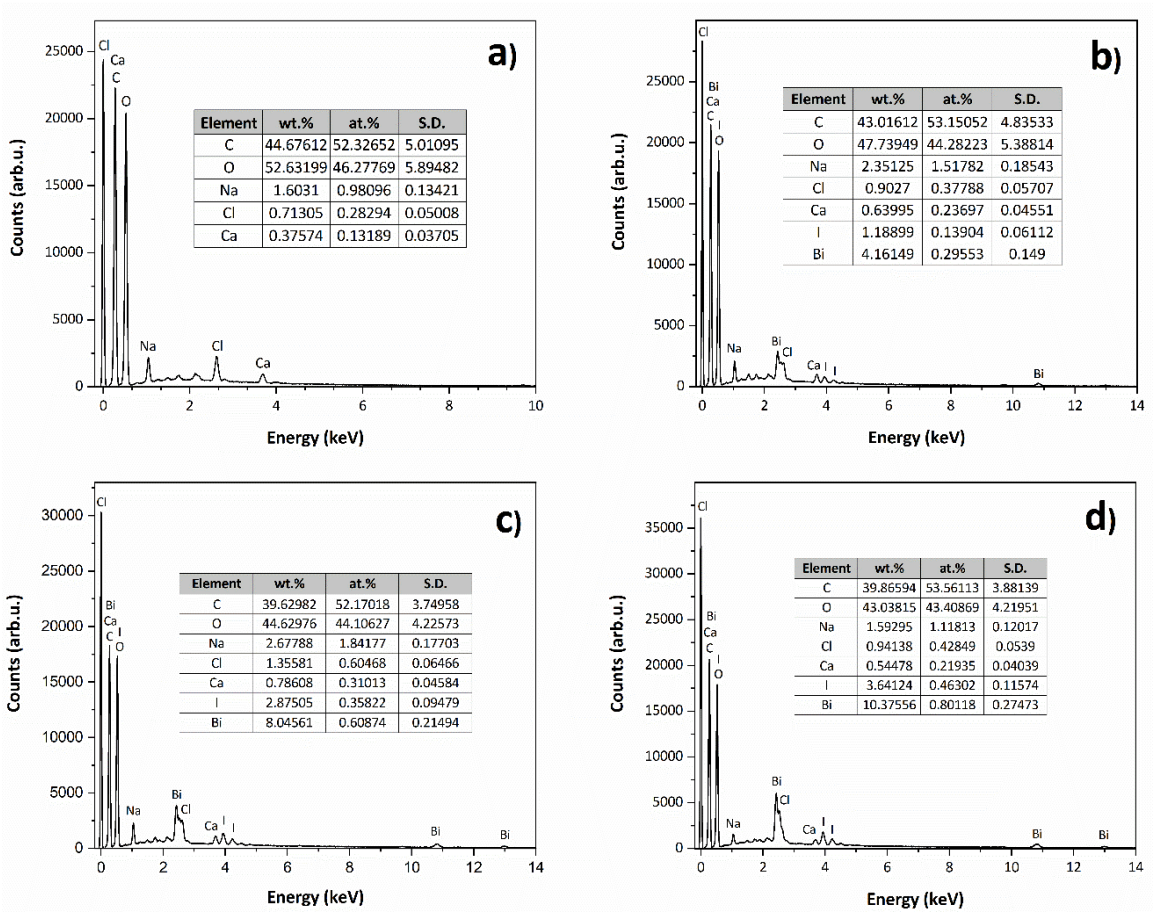

Fig. 3. EDS images of HC/BiOI-0 (a), HC/BiOI-50 (b), HC/BiOI-100 (c), and HC/BiOI-200 (d) samples.

Additionally, as seen in Fig. 3b-d, an increase in the weight percentage of Bi and I is observed as the dose of microspheres inside the membrane is increased. For the functionalized samples, HC/BiOI-50 exhibits 4.161% for Bi and 1.189% for I. In the case of HC/BiOI-100, the percentages are 8.046% for Bi and 2.875% for I. Finally, for HC/BiOI-200, the values reach 10.386% for Bi and 3.641% for I. Therefore, this could indicate the effectiveness of the functionalization process. Moreover, these results are consistent with XRD results, in which the intensity of characteristic BiOI peaks also increases by increasing the amount of BiOI microspheres. Therefore, this indicates that BiOI microspheres were effectively incorporated into the cellulose membrane matrix.

3.2. Photocatalytic activity

The visible-light photocatalytic efficiency of the prepared samples was evaluated by monitoring the degradation of MB solution. Figure 4 depicts the results of dye removal efficiency using HC/BiOI-0, HC/BiOI-50, HC/BiOI-100, HC/BiOI-200, BiOI-50, BiOI-100 and BiOI-200 under two distinct conditions: in the presence of visible light and darkness conditions. The photolysis test shows a minimal removal of MB of only 13.33%. This is because, methylene blue (MB) is known to be a highly stable under visible light irradiation (I. Khan et al., 2022). Consequently, these results demonstrate that visible light irradiation, in the absence of photocatalysts, cannot significantly reduce the concentration of MB due to its inherent stability.

Under visible light conditions, the removal percentage for the unfunctionalized sample, HC/BiOI-0, was 82.85%. This effect can be attributed to two mechanisms: adsorption by hemp cellulose and photolysis induced by visible light. The adsorption capacity of the material is primarily due to the D-anhydroglucose molecular units linked by β-1,4 glycosidic bonds. Each unit contains three hydroxyl groups, which form intramolecular and intermolecular hydrogen bonds (Tofan et al., 2020). The presence of these hydroxyl groups imparts a negative surface charge, enabling effective adsorption of positively charged pollutants, such as methylene blue (a cationic dye), through electrostatic interaction. Furthermore, as seen in Fig. 2a, HC/BiOI-0 has a porous and fibrous structure, consisting of numerous cavities and voids, which provides a large surface area that can facilitate MB adsorption.

Regarding the hemp cellulose (HC) samples functionalized with BiOI, the obtained results demonstrate that the adsorption and photocatalytic efficiency varies significantly with the amount of BiOI used. The HC/BiOI-100 sample exhibited the highest performance achieving a removal of 93.67% of MB, suggesting that 100 mg of BiOI is the optimal dosage to maximize photocatalytic activity of hemp cellulose membranes. In contrast, HC/BiOI-50 exhibited a removal efficiency of 79.18%, indicating that an insufficient amount of BiOI microspheres may result in a low amount of available active sites on the photocatalytic surface for the degradation of the contaminant. On the other

hand, HC/BiOI-200 showed the lowest performance (70.71%), which could be related to the saturation or shielding effects caused by the excess of BiOI microspheres. That is, the microspheres could occupy some of the active adsorption sites on the membrane, thereby reducing the capacity to retain the dye. Moreover, as is shown in SEM images an excessive amount of BiOI microspheres caused their agglomeration, which means that the surface area to carry out the photocatalytic degradation of MB was likely decreased. Also, Geng et al. (2018) observed that the degradation efficiency for RhB increases much slower with increasing catalyst dosage, which could be attributed to the light shielding effect caused by the excessive amount of BiOI microspheres, for this case.

On the other hand, the figure shows the results obtained under dark conditions. For the HC/BiOI-0, a minimum methylene blue (MB) removal of 10.04% is recorded, indicating that the non-functionalised hemp cellulose has a low adsorption capacity in the dark. In the case of HC/BiOI-50, an increase in MB removal is observed, reaching a value of 27.30%. This suggests that the addition of 50 mg of BiOI microspheres improves the adsorption capacity in the dark. For HC/BiOI-100, the MB removal is 33.60%, which shows a slight increase compared to the previous sample. This indicates that the adsorption capacity continues to improve as the amount of BiOI increases, albeit gradually. Finally, for HC/BiOI-200, the removal decreases slightly to 31.14%. This suggests that an excessive amount of BiOI microspheres may begin to saturate the membrane, reducing the adsorption capacity of the material.

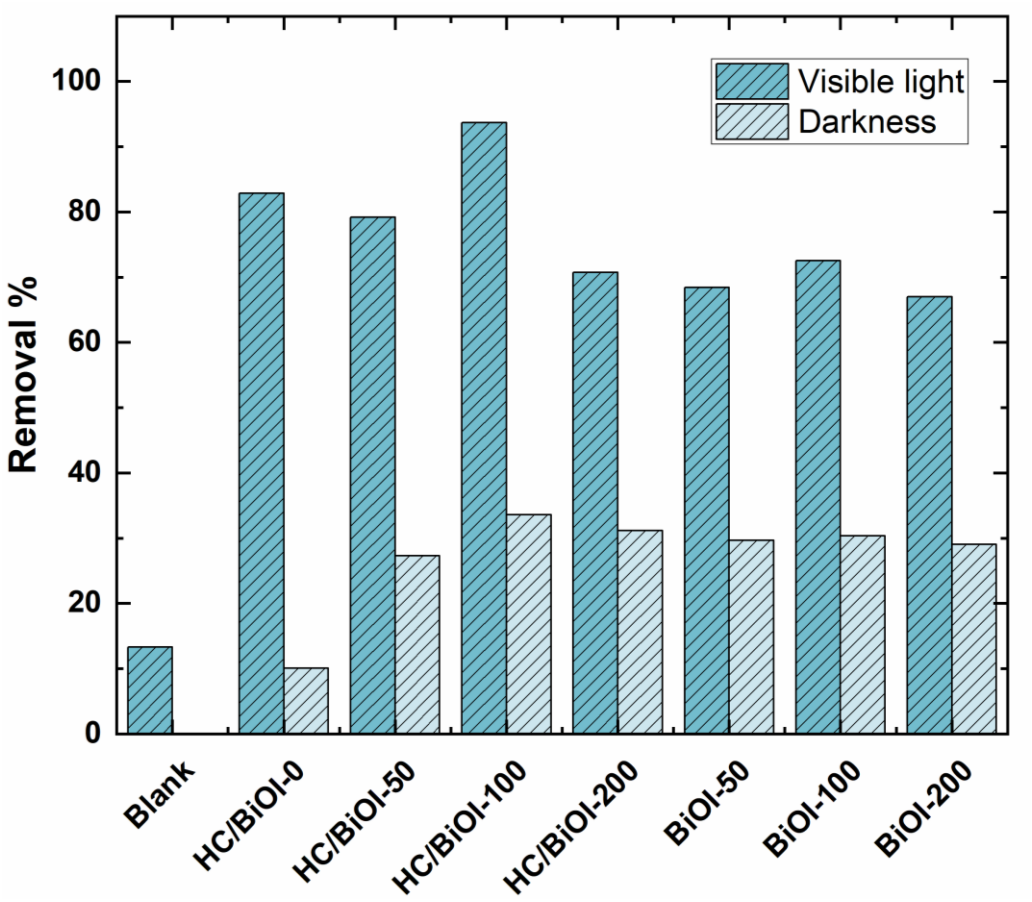

Fig. 4. Percentage of Methylene Blue Removal Under Visible Light and Dark Conditions.

On the other hand, in the case of BiOI-50, a removal of 29.68% is obtained, which is slightly higher than that of the HC/BiOI-50 sample, showing significant removal values under dark conditions. For BiOI-100 and BiOI-200 the removals are 30.37% and 29.01% respectively. Therefore, under these conditions, adsorption is the predominant mechanism for the removal of methylene blue (MB). Hemp cellulose (HC) alone exhibits adsorption capacity due to the presence of hydroxyl (-OH) groups, which form hydrogen bonds and facilitate electrostatic interaction with the cationic dye (MB). In addition, its porous and fibrous surface contributes to the adsorption of MB.

The incorporation of BiOI microspheres into the hemp cellulose membrane improves the adsorption capacity under dark conditions. Although BiOI is primarily a photocatalytic material, it also has some adsorption capacity. BiOI microspheres increase the surface area available for adsorption of methylene blue (MB), resulting in increased removal under these conditions. By increasing the amount of BiOI from 50 mg

to 100 mg, a slight increase in MB removal is observed, indicating that an adequate amount of BiOI improves the adsorption capacity. However, when the amount of BiOI is increased to 200 mg, the removal decreases slightly. This could be due to an excess of BiOI causing saturation of the active sites on the membrane or agglomeration of the material reducing the available contact area.

Finally, statistical analysis performed by one-way Analysis of Variance (ANOVA) reveals that both exposure time (in darkness and visible light: 60 min) and the dosage of BiOI used in the functionalization of hemp cellulose membranes have a significant effect on MB degradation (p-value = $<2e^{-16}$). The significant interaction between exposure time and BiOI amount indicates that the effectiveness of exposure time is linked to the amount of BiOI, suggesting a synergistic relationship. This interaction can be seen in Fig. 5, which shows how the optimal BiOI dosage varies with exposure time. Furthermore, the analysis supports the finding that an optimal BiOI dose (100 mg) maximizes MB removal (93.67%). Fig. 6 indicates that this intermediate dose presents the lowest final MB concentration, whereas an excessive BiOI amount (200 mg) may decrease efficiency due to saturation and light shielding effects. Additionally, Levene's test (p-value = 0.9906) and Shapiro-Wilk test (p-value = 0.2743) confirm that the data satisfy the assumptions required for the validity of the ANOVA analysis (Fig. S6).

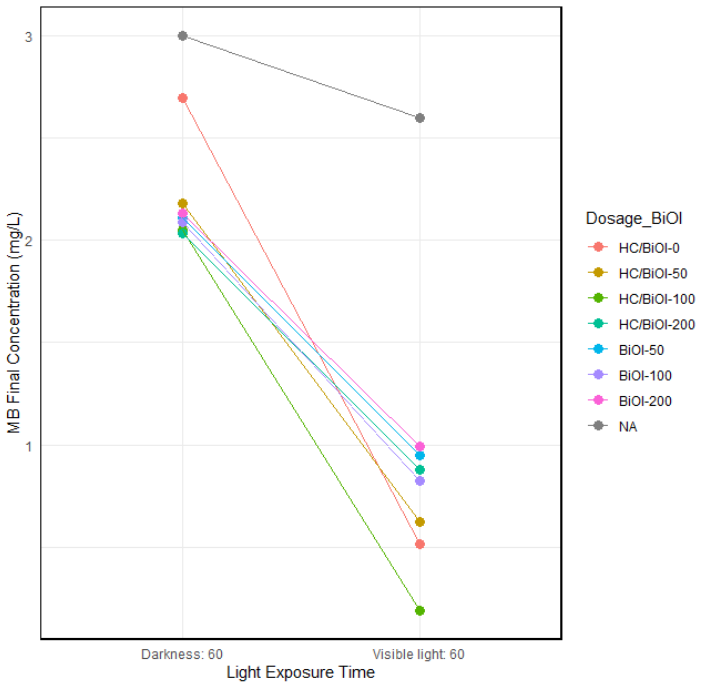

Fig. 5. Interaction plot: light exposure vs. BiOI dosage.

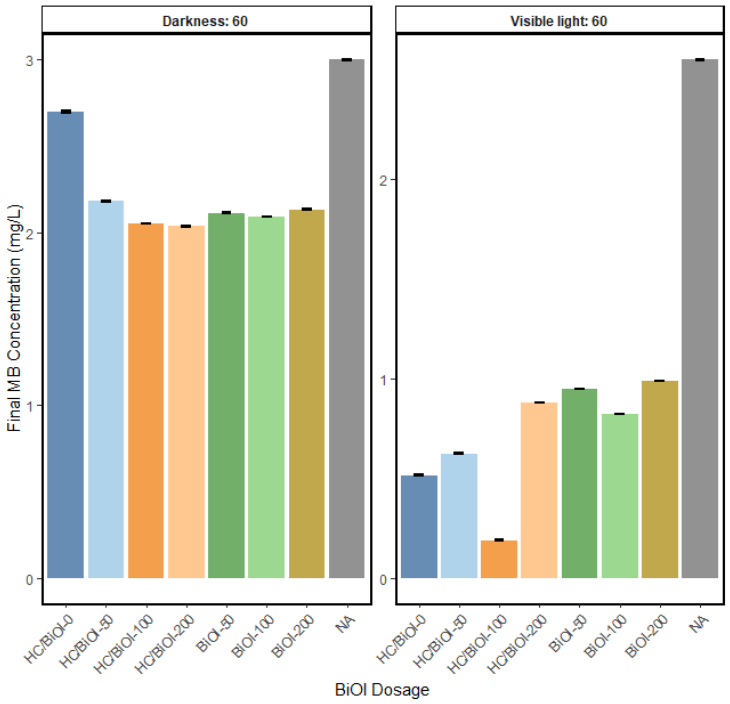

Fig. 6. Mean and Standard Deviation of final Methylene Blue Concentration.

4. CONCLUSIONS

Functionalization of hemp cellulose membranes with bismuth oxyiodide (BiOI) microspheres optimizes the degradation of methylene blue (MB) under visible light irradiation. The results indicate that incorporating BiOI improves the material's ability to degrade MB, suggesting that BiOI promotes the generation of reactive oxygen species (ROS) under visible light exposure.

The BiOI dosage plays a crucial role in optimizing the photocatalytic process. The results show that an intermediate amount of BiOI (100 mg) yielded the highest MB removal efficiency (93.67%), indicating the existence of an optimal BiOI loading for maximizing the photocatalytic activity of hemp cellulose membranes. On the other hand, a decrease in MB removal efficiency was observed in samples with a higher amount of BiOI (200 mg), which is attributed to a saturation and light shielding effect. This phenomenon indicates that an excess of photocatalytic material can block the active sites and reduce the availability of light needed to initiate the photocatalytic process, thus limiting its efficiency.

The functionalization of hemp cellulose with BiOI microspheres proves to be an effective strategy for the removal of methylene blue, highlighting the importance of using the correct amount of BiOI to optimise the degradation efficiency of the pollutant. This research supports the idea that combining biodegradable materials, such as hemp cellulose, with effective photocatalysts offers a viable and sustainable approach to wastewater decontamination. This approach stands out as a more sustainable alternative to traditional methods that often generate secondary waste or incur high operating costs, highlighting the potential of these materials in wastewater treatment applications.

5. FUNDING SOURCES

This research was funded by the following contributions: Ecuadorian Corporation for the Development of Research and Academia (CEDIA) (Grant No: CEPRA XVI-2022–21 CONTAMINANT DEGRADATION). Erasmus+ CBHE Consortium "NB-LAB" (Grant No: 619346–EPP–1–2020–1–DE –EPPKA2–CBHE–JP) and Ikiam Territory Project Call 2024 (Registration Code: DIFCSA-001-2024).

6. ACKNOWLEDGMENTS

We thank Regina Krause (Hochschule Wismar), Gabriela Montealegre (CEDIA), and the Research Directorate of the Amazon Regional University Ikiam for their logistical support, as well as CENCINAT of the Armed Forces University ESPE and the Institute of Energy and Materials of USFQ.

7. AUTHOR CONTRIBUTIONS: CREDIT

Kerly Jamileth Díaz Solórzano: Conceptualization, Data curation, Methodology, Investigation, Writing – original draft. **Leonardo Proaño:** review & editing. **Maria Auquilla:** review & editing. **Michael Zuarez-Chamba:** review & editing. **Frank Alexis:** Investigation, Methodology, review & editing. **Karla Vizuete:** Investigation, Writing – review & editing. **Alexis Debut:** Investigation, Writing – review & editing. **Miguel Quishpe:** Conceptualization, Supervision, Funding acquisition, Writing – review & editing. **Miguel Herrera-Robledo:** Supervision, Funding acquisition, Writing – review & editing

8. REFERENCES

Akköz, Y., & Coşkun, R. (2023). Cellulose-supported bioadsorbent from natural hemp fiber for removal of anionic dyes from aqueous solution. *International Journal of Biological Macromolecules*, *252*, 126447. https://doi.org/10.1016/j.ijbiomac.2023.126447

Ara, M., & Ghafuri, H. (2024). Design and preparation of a novel Mg–Al LDH@EDTA-Melamine nanocomposite for effective adsorptive removal of methylene blue and rhodamine B dyes from water. *Heliyon*, *10*(12), e32447. https://doi.org/10.1016/j.heliyon.2024.e32447

Basak, A. K., R, A., Benzegar, A., Agunde, R., & Dinakar, S. (2015). Absorption of anthocyanin dye and its first order kinetics on bacterial cellulose produced by fermentation of black tea. *IOSR Journal of Biotechnology and Biochemistry*, *1*(4), 28-32.

Bokuniaeva, A. O., & Vorokh, A. S. (2019). Estimation of particle size using the Debye equation and the Scherrer formula for polyphasic TiO2 powder. *Journal of Physics: Conference Series*, *1410*(1), 012057. https://doi.org/10.1088/1742-6596/1410/1/012057

Bolio, G., Valadez, A., Veleva, L., & Andreeva, A. (2011). Whiskers de celulosa a partir de residuos agroindustriales de banano: Obtención y caracterización. *Revista mexicana de ingeniería química*, *10*, 291-299.

Candamano, S., Coppola, G., Mazza, A., Caicho Caranqui, J. I., Bhattacharyya, S., Chakraborty, S., Alexis, F., & Algieri, C. (2023). Batch and fixed bed adsorption of methylene blue onto foamed metakaolin-based geopolymer: A preliminary investigation. *Chemical Engineering Research and Design*, *197*, 761-773. https://doi.org/10.1016/j.cherd.2023.08.014

Chen, J., Wang, X., Long, Z., Wang, S., Zhang, J., & Wang, L. (2020). Preparation and performance of thermoplastic starch and microcrystalline cellulose for packaging composites: Extrusion and hot pressing. *International Journal of Biological Macromolecules*, *165*, 2295-2302. https://doi.org/10.1016/j.ijbiomac.2020.10.117

Di, J., Xia, J., Li, H., Guo, S., & Dai, S. (2017). Bismuth oxyhalide layered materials for energy and environmental applications. *Nano Energy*, *41*, 172-192. https://doi.org/10.1016/j.nanoen.2017.09.008

Du, M., Du, Y., Feng, Y., Li, Z., Wang, J., Jiang, N., & Liu, Y. (2019). Advanced photocatalytic performance of novel BiOBr/BiOI/cellulose composites for the removal of organic pollutant. *Cellulose*, *26*(9), 5543-5557. https://doi.org/10.1007/s10570-019-02474-1

Du, M., Du, Y., Feng, Y., Yang, K., Lv, X., Jiang, N., & Liu, Y. (2018). Facile preparation of BiOBr/cellulose composites by in situ synthesis and its enhanced photocatalytic activity under visible-light. *Carbohydrate Polymers*, *195*, 393-400. https://doi.org/10.1016/j.carbpol.2018.04.092

Du, S., Zhao, Z., Li, B., Li, Y., Tong, N., Che, Q., & Wang, J. (2024). Preparation of natural antibacterial regenerated cellulose fiber from seed-type hemp. *Industrial Crops and Products*, *208*, 117873. https://doi.org/10.1016/j.indcrop.2023.117873

Ekeoma, B. C., Ekeoma, L. N., Yusuf, M., Haruna, A., Ikeogu, C. K., Merican, Z. M. A., Kamyab, H., Pham, C.

Q., Vo, D. V. N., & Chelliapan, S. (2023). Recent advances in the biocatalytic mitigation of emerging pollutants: A comprehensive review. *Journal of Biotechnology*, *369*, 14-34. https://doi.org/10.1016/J.JBIOTEC.2023.05.003

Figueroa, F. (2020). *Remediación de la contaminación de agua por metales pesados con el uso de celulosa de la biodiversidad de Ecuador* [Tesis, Universidad de Investigación de Tecnología Experimental Yachay]. http://repositorio.yachaytech.edu.ec/handle/123456789/180

Fito, J., Abewaa, M., Mengistu, A., Angassa, K., Ambaye, A. D., Moyo, W., & Nkambule, T. (2023). Adsorption of methylene blue from textile industrial wastewater using activated carbon developed from Rumex abyssinicus plant. *Scientific Reports*, *13*(1), 5427. https://doi.org/10.1038/s41598-023-32341-w

Fito, J., Abrham, S., & Angassa, K. (2020). Adsorption of Methylene Blue from Textile Industrial Wastewater onto Activated Carbon of Parthenium hysterophorus. *International Journal of Environmental Research*, *14*(5), 501-511. https://doi.org/10.1007/s41742-020-00273-2

Gao, X., Dai, J., Zhang, Q., & Li, H. (2023). An advanced oxidized bacterial cellulose platform for improving the photocatalysis performance of BiOCl. *Materials Today Communications*, *37*, 1-12. https://doi.org/10.1016/j.mtcomm.2023.107030

Geng, A., Meng, L., Han, J., Zhong, Q., Li, M., Han, S., Mei, C., Xu, L., Tan, L., & Gan, L. (2018). Highly efficient visible-light photocatalyst based on cellulose derived carbon nanofiber/BiOBr composites. *Cellulose*, *25*(7), 4133-4144. https://doi.org/10.1007/s10570-018-1851-y

Gordon-Falconí, C., Iannone, M. F., Zawoznik, M. S., Debut, A., & Groppa, M. D. (2024). Discarded yerba mate as a source of cellulose fibers with promising applications for drinking water decontamination. *Industrial Crops and Products*, *211*, 118253. https://doi.org/10.1016/j.indcrop.2024.118253

Hashem, A. H., Saied, E., & Hasanin, M. S. (2020). Green and ecofriendly bio-removal of methylene blue dye from aqueous solution using biologically activated banana peel waste. *Sustainable Chemistry and Pharmacy*, *18*, 100333. https://doi.org/10.1016/j.scp.2020.100333

Hermans, P. H., & Weidinger, A. (1948). Quantitative X-Ray Investigations on the Crystallinity of Cellulose Fibers. A Background Analysis. *Journal of Applied Physics*, *19*(5), 491-506. https://doi.org/10.1063/1.1698162

Hokkanen, S., Bhatnagar, A., & Sillanpää, M. (2016). A review on modification methods to cellulose-based adsorbents to improve adsorption capacity. *Water Research*, *91*, 156-173. https://doi.org/10.1016/j.watres.2016.01.008

Houas, A., Lachheb, H., Ksibi, M., Elaloui, E., Guillard, C., & Herrmann, J.-M. (2001). Photocatalytic degradation pathway of methylene blue in water. *Applied Catalysis B: Environmental*, *31*(2), 145-157. https://doi.org/10.1016/S0926-3373(00)00276-9

Kausar, A., Zohra, S. T., Ijaz, S., Iqbal, M., Iqbal, J., Bibi, I., Nouren, S., Messaoudi, N. E., & Nazir, A. (2023). Cellulose-based materials and their adsorptive removal efficiency for dyes: A review. *International Journal of Biological Macromolecules*, *224*, 1337-1355.

https://doi.org/10.1016/J.IJBIOMAC.2022.10.220

Khan, I., Saeed, K., Zekker, I., Zhang, B., Hendi, A. H., Ahmad, A., Ahmad, S., Zada, N., Ahmad, H., Shah, L. A., Shah, T., & Khan, I. (2022). Review on Methylene Blue: Its Properties, Uses, Toxicity and Photodegradation. *Water 2022, Vol. 14, Page 242*, *14*(2), 1-30. https://doi.org/10.3390/W14020242

Khan, S., Naushad, M., Govarthanan, M., Iqbal, J., & Alfadul, S. M. (2022). Emerging contaminants of high concern for the environment: Current trends and future research. *Environmental Research*, *207*, 1-17. https://doi.org/10.1016/J.ENVRES.2021.112609

Li, Y., Jiang, H., Wang, X., Hong, X., & Liang, B. (2021). Recent advances in bismuth oxyhalide photocatalysts for degradation of organic pollutants in wastewater. *RSC Advances*, *11*(43), 26855-26875. https://doi.org/10.1039/D1RA05796K

Mahfoudhi, N., & Boufi, S. (2017). Nanocellulose as a novel nanostructured adsorbent for environmental remediation: A review. *Cellulose*, *24*(3), 1171-1197. https://doi.org/10.1007/s10570-017-1194-0

Mohamed, M. A., Abd Mutalib, M., Mohd Hir, Z. A., M. Zain, M. F., Mohamad, A. B., Jeffery Minggu, L., Awang, N. A., & W. Salleh, W. N. (2017). An overview on cellulose-based material in tailoring bio-hybrid nanostructured photocatalysts for water treatment and renewable energy applications. *International Journal of Biological Macromolecules*, *103*, 1232-1256. https://doi.org/10.1016/j.ijbiomac.2017.05.181

Negrete-Bolagay, D., Zamora-Ledezma, C., Chuya-Sumba, C., De Sousa, F. B., Whitehead, D., Alexis, F., & Guerrero, V. H. (2021). Persistent organic pollutants: The trade-off between potential risks and sustainable remediation methods. *Journal of Environmental Management*, *300*, 113737. https://doi.org/10.1016/j.jenvman.2021.113737

Nor, N. A. M., Jaafar, J., Ismail, A. F., Mohamed, M. A., Rahman, M. A., Othman, M. H. D., Lau, W. J., & Yusof, N. (2016). Preparation and performance of PVDF-based nanocomposite membrane consisting of TiO2 nanofibers for organic pollutant decomposition in wastewater under UV irradiation. *Desalination*, *391*, 89-97. https://doi.org/10.1016/j.desal.2016.01.015

Oladoye, P. O., Ajiboye, T. O., Omotola, E. O., & Oyewola, O. J. (2022). Methylene blue dye: Toxicity and potential elimination technology from wastewater. *Results in Engineering*, *16*, 1-17. https://doi.org/10.1016/J.RINENG.2022.100678

Onwumere, J., Piątek, J., Budnyak, T., Chen, J., Budnyk, S., Karim, Z., Thersleff, T., Kuśtrowski, P., Mathew, A. P., & Slabon, A. (2020). CelluPhot: Hybrid Cellulose-Bismuth Oxybromide Membrane for Pollutant Removal. *ACS Applied Materials and Interfaces*, *12*(38), 42891-42901. https://doi.org/10.1021/ACSAMI.0C12739/ASSET/IMAGES/LARGE/AM0C12739_0010.JPEG

Patel, N., Khan, MD. Z. A., Shahane, S., Rai, D., Chauhan, D., Kant, C., & Chaudhary, V. K. (2020). Emerging Pollutants in Aquatic Environment: Source, Effect, and Challenges in Biomonitoring and Bioremediation- A Review. *Pollution*, *6*(1), 99-113. https://doi.org/10.22059/poll.2019.285116.646

Poletto, M., Ornaghi, H. L., & Zattera, A. J. (2014). Native Cellulose: Structure, Characterization and

Thermal Properties. *Materials*, *7*(9), Article 9. https://doi.org/10.3390/ma7096105

Santoso, E., Ediati, R., Kusumawati, Y., Bahruji, H., Sulistiono, D. O., & Prasetyoko, D. (2020). Review on recent advances of carbon based adsorbent for methylene blue removal from waste water. *Materials Today Chemistry*, *16*, 100233. https://doi.org/10.1016/j.mtchem.2019.100233

Sivakumar, R., & Lee, N. Y. (2022). Adsorptive removal of organic pollutant methylene blue using polysaccharide-based composite hydrogels. *Chemosphere*, *286*, 131890. https://doi.org/10.1016/j.chemosphere.2021.131890

Tofan, L., Paduraru, C., & Teodosiu, C. (2020). Hemp Fibers for Wastewater Treatment. En G. Crini & E. Lichtfouse (Eds.), *Sustainable Agriculture Reviews 42* (Vol. 42, pp. 295-326). Springer International Publishing. https://doi.org/10.1007/978-3-030-41384-2_10

Wang, X., Li, X., Wang, X., Zhao, M., Chen, W., Wu, H., & Jia, J. (2022). Immobilization of bismuth oxychloride on cellulose nanocrystal for sunlight-driven superior photosensitized degradation. *International Journal of Biological Macromolecules*, *206*, 398-408. https://doi.org/10.1016/j.ijbiomac.2022.02.159

Xu, M., Deng, Y., Li, S., Zheng, J., Liu, J., Tremblay, P.-L., & Zhang, T. (2023). Bacterial cellulose flakes loaded with Bi2MoO6 nanoparticles and quantum dots for the photodegradation of antibiotic and dye pollutants. *Chemosphere*, *312*, 137249. https://doi.org/10.1016/j.chemosphere.2022.137249

Zuarez-Chamba, M., Tuba-Guamán, D., Quishpe, M., Vizuete, K., Debut, A., & Herrera-Robledo, M. (2022). Photocatalytic degradation of bisphenol A on BiOI nanostructured films under visible LED light irradiation. *Journal of Photochemistry and Photobiology A: Chemistry*, *431*, 1-10. https://doi.org/10.1016/j.jphotochem.2022.114021

9. SUPPLEMENTARY MATERIAL

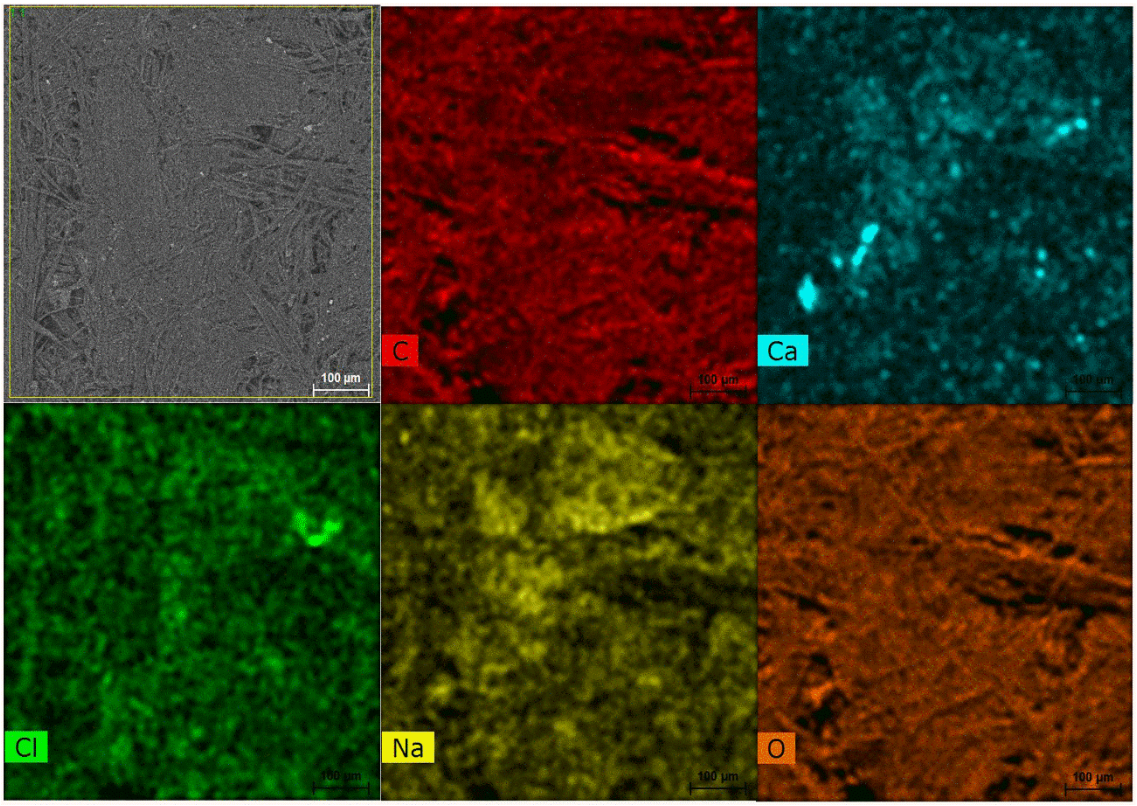

Fig. S1. Mapping of HC/BiOI-0 sample

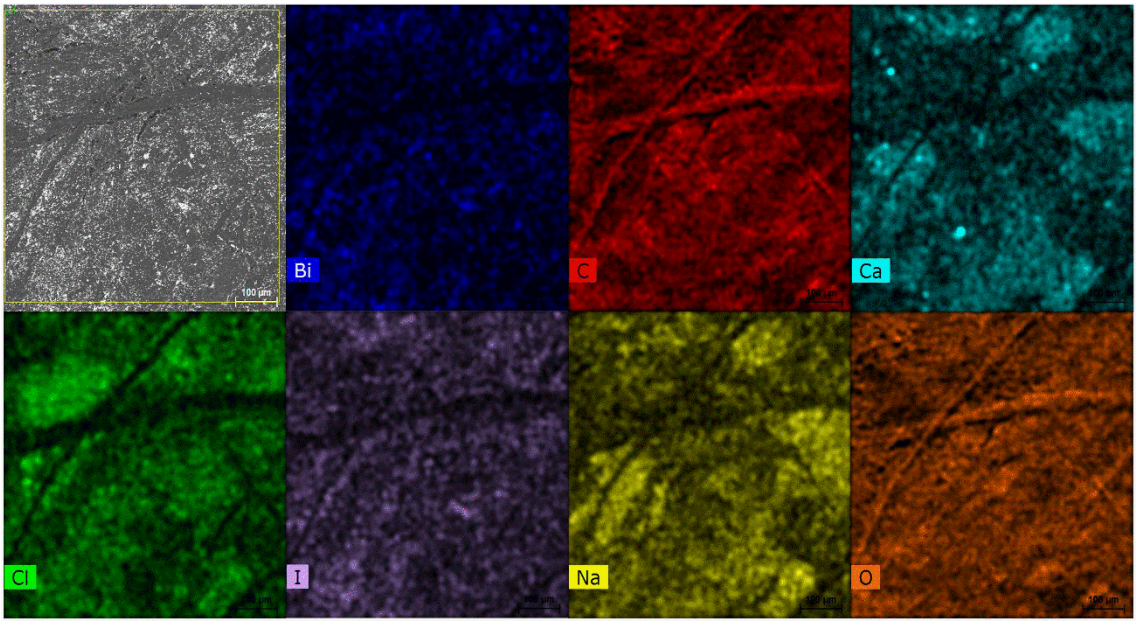

Fig. S2. Mapping of HC/BiOI-50 sample

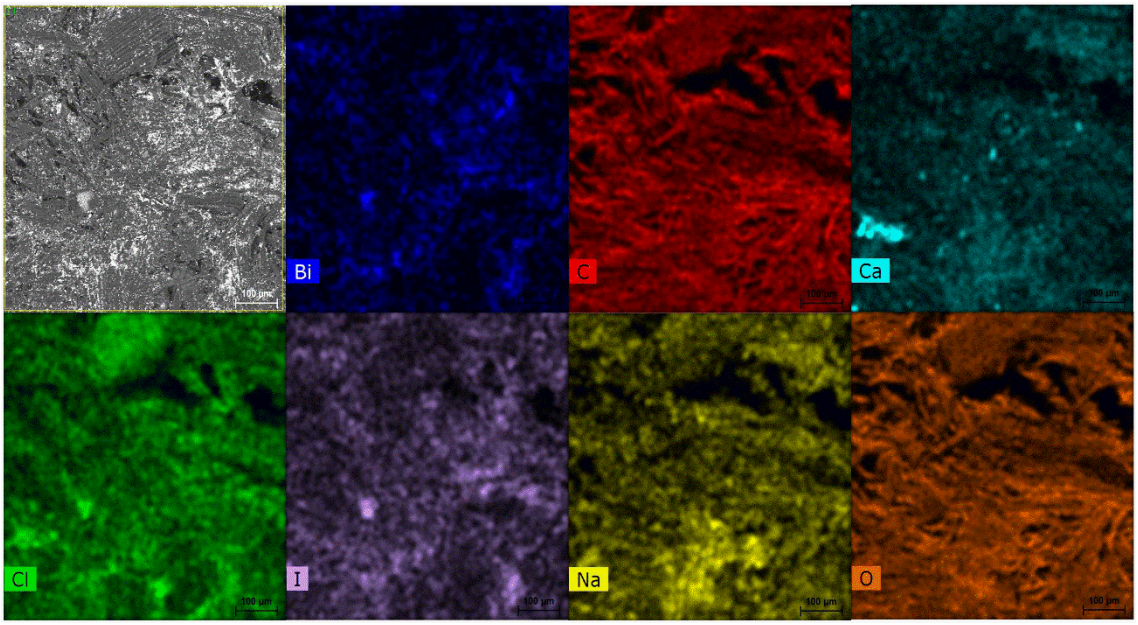

Fig. S3. Mapping of HC/BiOI-100 sample

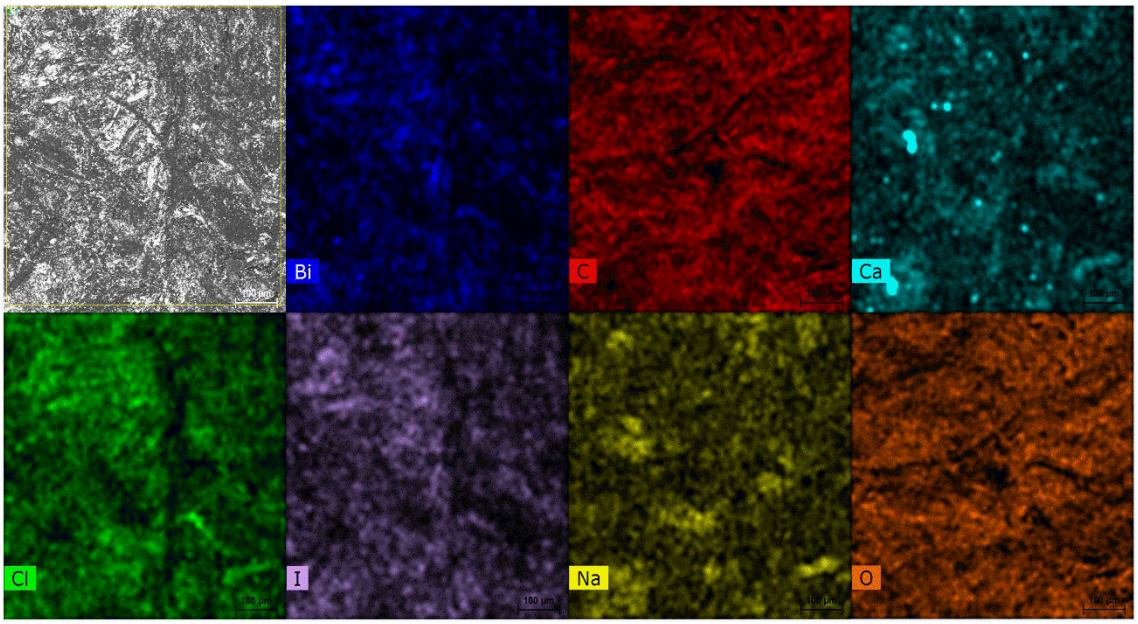

Fig. S4. Mapping of HC/BiOI-200 sample

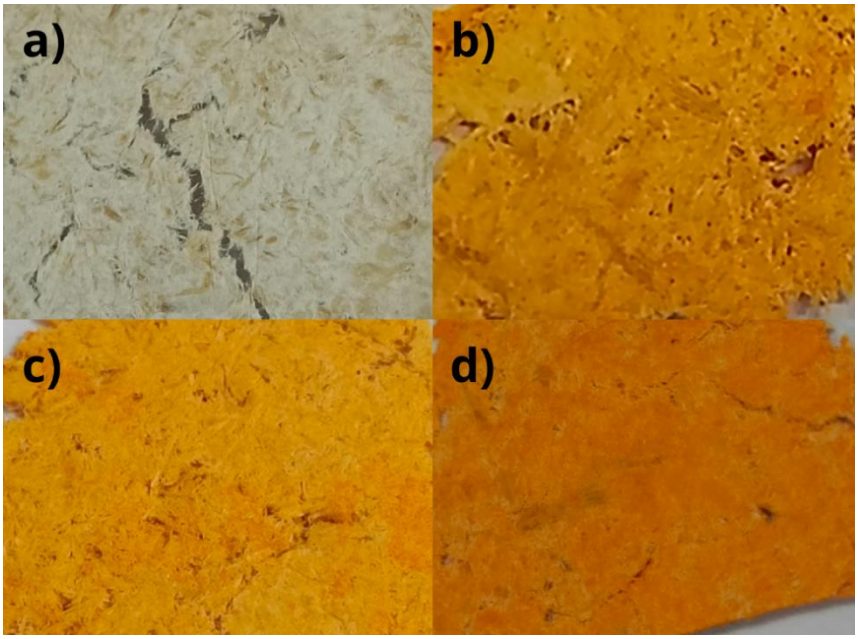

Fig. S5. Photographs of the membranes, (a) HC/BiOI-0, (b) HC/BiOI-50, (c) HC/BiOI-100 and (d) HC/BiOI-200.

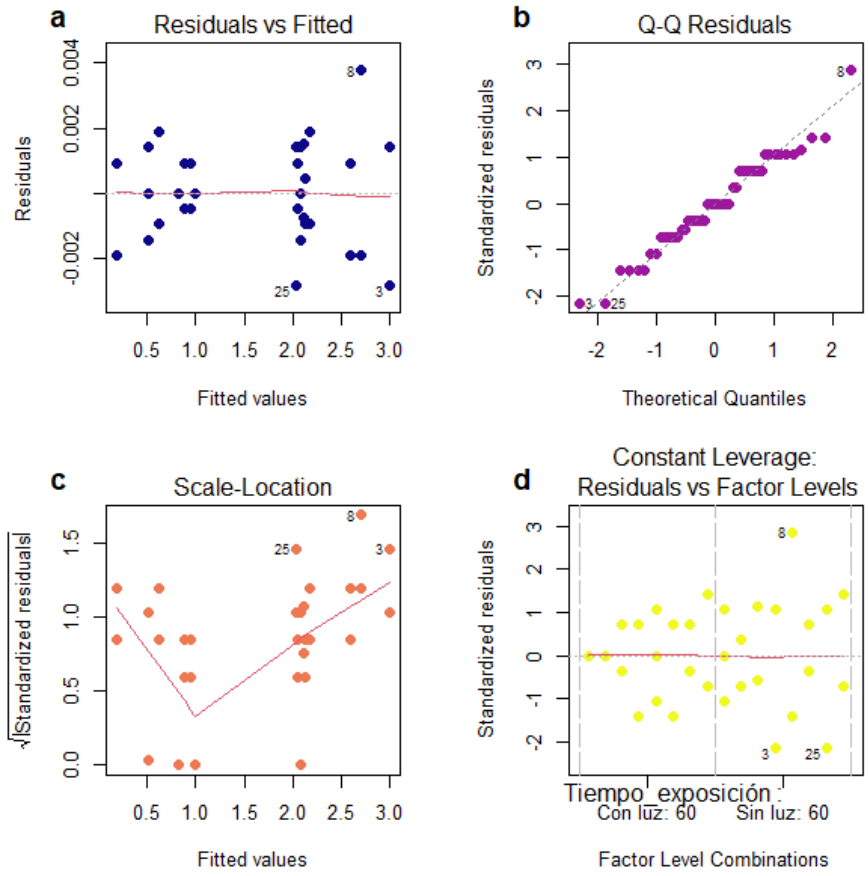

Fig. S6. Diagram of residuals